Electronic Supplementary Material (ESI) for Catalysis Science & Technology.

Supporting Information

Greatly enhanced photocatalytic activity by organic flexible piezoelectrics PVDF induced spatial electric field

Baoying Dai[a,b,c], Hengming Huang[a,b,c], Wei Wang[d], Yukai Chen[a,b,c], Chunhua Lu[a,b,c]*, Jiahui Kou[a,b,c]*, Lianzhou Wang[e], Fulei Wang[f] and Zhongzi Xu[a,b,c]

[a] State Key Laboratory of Materials-Oriented Chemical Engineering, College of Materials Science and Engineering, Nanjing Tech University, Nanjing 210009, P. R. China.

[b] Jiangsu Collaborative Innovation Center for Advanced Inorganic Function Composites, Nanjing Tech University, Nanjing 210009, P. R. China.

[c] Jiangsu National Synergetic Innovation Center for Advanced Materials (SICAM), Nanjing Tech University, Nanjing 210009, P. R. China.

[d] School of Physics and Optoelectronic Engineering, Nanjing University of Information Science & Technology, Nanjing 210044, P. R. China.

[e] Nanomaterials Center, School of Chemical Engineering and Australia Institute for Bioengineering and Nanotechnology, University of Queensland, Brisbane, Queensland 4072, Australia

[f] State Key Laboratory of Crystal Materials, Shandong University, Jinan, 250100, PR China

Corresponding authors:
* E-mail: chhlu@njtech.edu.cn (C. L.), Tel: +86-25-83587252.
* E-mail: jhkou@njtech.edu.cn (J. K.).

Supplementary text

1 Materials

Tantalum (Ⅴ) oxide (Ta_2O_5, 99.99%, Aladdin) and sodium hydroxide (NaOH, 96%，Xilong Chemical Co., Ltd) were selected to prepare sodium tantalate ($NaTaO_3$) powders. Nitric acid (HNO_3, 65.0~68.0%, Shanghai Lingfeng Chemical Reagent CO., Ltd.), bismuth (Ⅲ) nitrate pentahydrate ($Bi(NO_3)_3 \cdot 5H_2O$, ≥99.0%, Sinopharm Chemical Reagent Co., Ltd), ammonium metavanadate (NH_4VO_3, ≥99.0%, Sinopharm Chemical Reagent Co., Ltd) and ammonia solution ($NH_3 \cdot H_2O$, 25~28%, Shanghai Lingfeng Chemical Reagent CO., Ltd.) were used to synthesize bismuth vanadate ($BiVO_4$) sample. Urea (CON_2H_4, 99%, Xilong Chemical Co., Ltd）was utilized to fabricate graphitic carbon nitride (g-C_3N_4).

2 Methods

2.1 Preparation of $NaTaO_3$, $BiVO_4$ and g-C_3N_4.

As we know, $NaTaO_3$, as a representative UV-light-responsive catalyst, exhibiting significant negative conduction band and great photocatalytic stability, has attracted a great deal of attention during the decades.[1, 2] $BiVO_4$ is famous for its application in water splitting and organic pollution degradation under visible light irradiation, which is ascribed to its relatively narrow bandgap and high catalytic efficiency.[3-6] Polymeric-based g-C_3N_4 is a new efficient visible-light-responsive photocatalyst. It has become a very hot research topic since the pioneering work in 2009.[7-9] Therefore, to investigate the generic enhancement effect of spatial electric field of PVDF on photocatalysis, it is representative and imperative to prepare the abovementioned three photocatalysts and combine them with PVDF, respectively.

$NaTaO_3$: $NaTaO_3$ was synthesized via a typical hydrothermal method.[10] 8.00 g

NaOH powders were dissolved in 20 mL of distilled water, and then 0.25 g of Ta_2O_5 powders were added. The obtained mixture was poured into a homemade polytetrafluoroethylene (PPL) lined stainless steel reactor with the capacity of 40 mL. After heated at 120 ^oC for 48 h, the product was centrifuged, washed with distilled water, and then dried at 60 ^oC in an oven overnight.

$BiVO_4$: Hydrothermal procedure was adopted to prepare $BiVO_4$ sample.[11] 4.21 g of NH_4VO_3 and 17.46 g of $Bi(NO_3)_3·5H_2O$ powders were dissolved in 220 mL and 80 mL 2 M HNO_3 solution, respectively. Then $Bi(NO_3)_3·5H_2O$ solution was drop-added into NH_4VO_4 solution under continuous stirring. Subsequently, 1 M $NH_3·H_2O$ was added to adjust pH value of the reaction mixture to 2 with vigorous stirring and vivid yellow precipitates were formed simultaneously. 70 mL of reaction product was taken out from the obtained precipitates after 6 h's standing and transferred into a 100 mL PPL lined stainless steel autoclave, the reaction was conducted at 200 ^oC for 24 h. Finally, the product was centrifuged, washed with distilled water and ethanol for several times and dried at 60 ^oC overnight.

g-C_3N_4: g-C_3N_4 was fabricated by directly heating urea in a muffle furnace.[12, 13] In detail, 20.00 g of precursor urea powders were put into a 100 mL alumina crucible with a cover after ground with a mortar. Then the alumina crucible was moved in a muffle furnace and heated at 520 ^oC for 4 h in air with the ramp rate of 25 ^oC/min. Finally, the obtained powders were ground before characterization and utilization.

2.2 Fabrication of photocatalytic films.

For comparison, the as-prepared photocatalysts were combined with PDMS and PVDF, respectively. The fabrication procedures of PVDF-$NaTaO_3$, PVDF-$BiVO_4$ and PVDF-g-C_3N_4 were similar to that of PVDF-TiO_2 except the content of $NaTaO_3$, $BiVO_4$ and g-C_3N_4 powders contained in the film is 0.50 g, respectively. Similarly, 0.50 g of photocatalysts $NaTaO_3$, $BiVO_4$ and g-C_3N_4 were combined with PDMS by the same preparation process as that of PDMS-TiO_2 to prepare PDMS-$NaTaO_3$, PDMS-$BiVO_4$ and PDMS-g-C_3N_4 films, respectively.

2.3 Photocatalytic performance measurement

To investigate the generic promotion effect of spatial electric field on photocatalysis, the photodegradation experiments of RhB over the prepared films were also conducted in a similar way as that of PVDF-TiO_2 and PDMS-TiO_2. During the photocatalytic reaction, a 300 W xenon lamp was employed as light source for PVDF-$BiVO_4$, PDMS-$BiVO_4$, PVDF-g-C_3N_4 and PDMS-g-C_3N_4 films, and the lamp equipped with a 420 nm cutoff filter was utilized to irradiate PVDF-$NaTaO_3$ and PDMS- $NaTaO_3$ films.

3 Results and discussion

3.1 Piezoelectric force microscope (PFM) of PVDF and PVDF-TiO_2 films

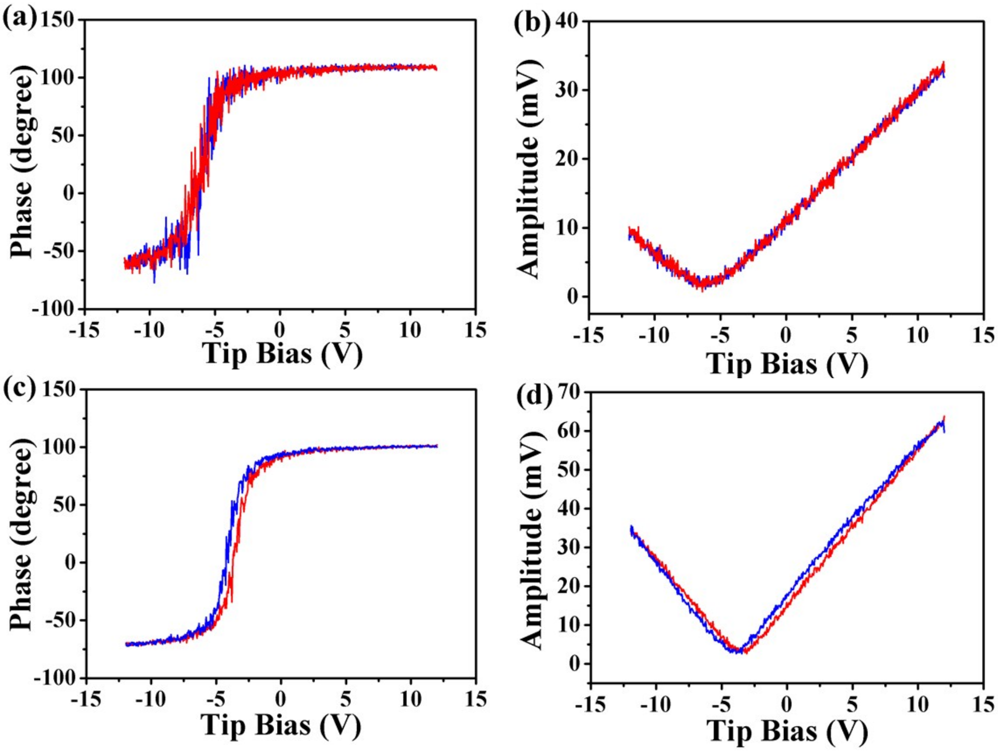

Fig. S1 Piezoelectric hysteresis and butterfly loops of films: pure PVDF (a, b) and PVDT-TiO_2 (c, d).

PFM is an effective technique to characterize piezoelectric property. Therefore, the piezoelectric hysteresis and butterfly loops of PVDF and PVDF-TiO_2 films were carried out using a Bruker Dimension Icon Scanning Probe Microscope with a Pt-coated conductive tip to study the influence of TiO_2 on the piezoelectric property of PVDF substrate. As Fig. S1 (a) and (b) displays, no typical square phase hysteresis loop and butterfly loop over PVDF are detected. It indicates that the piezoelectric property of pure PVDF film is poor. After combined with TiO_2, the slight square phase hysteresis and butterfly loop of PVDF-TiO_2 are attained, shown in Fig. S1 (c) and (d). It demonstrates that the piezoelectric property of PVDF is improved in the presence of TiO_2 nano particles.

3.2 Hydroxyl radical generation analysis

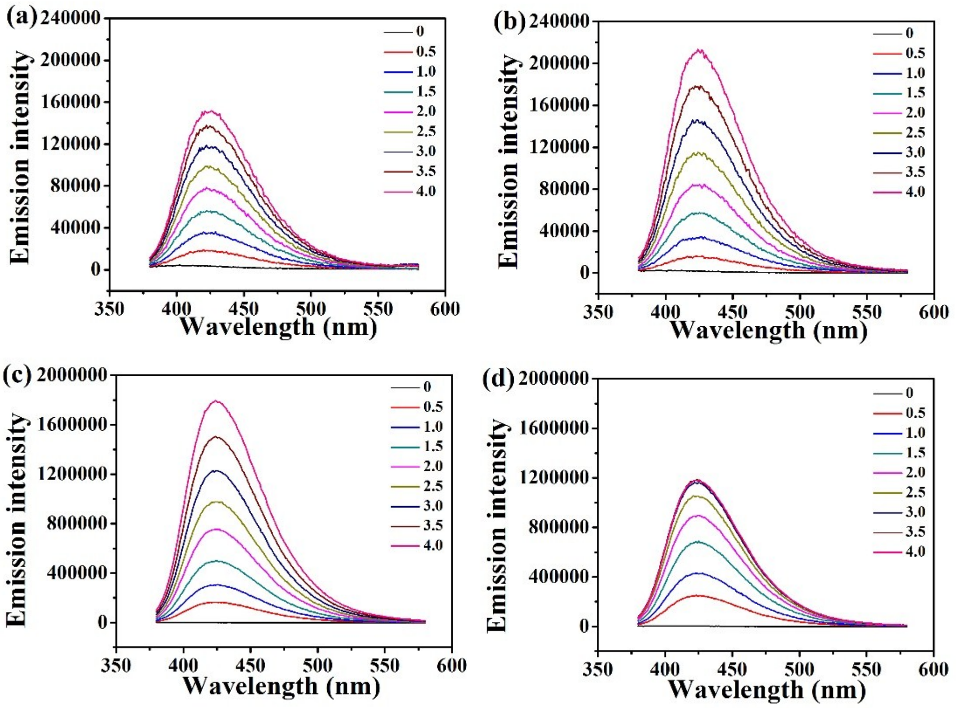

Fig. S2 Hydroxyl radical generation ability analysis spectra of TA in NaOH solution excited at 315 nm in the condition of U-L (over PVDF-TiO_2 (a) and PDMS-TiO_2 (b)) and S-L (over PVDF-TiO_2 (c) and PDMS-TiO_2 (d)), respectively.

As we know, hydroxyl radicals are the oxidation product of photogenerated holes and absorbed water, which can be trapped by terephthalic acid (TA) and produce 2-hydroxyterephthalic acid, a high fluorescence compound. Therefore, the PL intensity of 2-hydroxyterephthalic acid could be employed as a probe to detect the generation of hydroxyl radicals and effective photogenerated holes, the higher PL intensity indicates more effective photogenerated holes introduced into reaction system. In this work, significant PL spectra excited at 315 nm in NaOH solution of TA were observed and depicted in Fig. S2. The peaks centered at ca. 425 nm increase with reaction time. As displayed in Fig. S2 (a) and (b), the PL intensity of 2-

hydroxyterephthalic acid over PVDF-TiO_2 and PDMS-TiO_2 with the assistance of S-L in 4 h is 160000 and 220000, respectively. The similar PL intensity over PVDF-TiO_2 and PDMS-TiO_2 suggests that there is no big difference on the amounts of effective photogenerated holes of TiO_2 over PVDF-TiO_2 and PDMS-TiO_2 films, implying the similar photocatalytic efficiency of the films. The result is in good agreement with the catalytic degradation of RhB over two films under S-L. Moreover, the PL intensity at 425 nm over PVDF-TiO_2 in 4 h is up to 1800000, which is 1.5 times higher than that over PDMS-TiO_2 1200000 under U-L (Fig. S2 (c) and (d)). It verifies that the amounts of effective photogenerated holes of PVDF-TiO_2 are much more than that of PDMS-TiO_2 in the condition of U-L, indicating more superior photocatalytic activity of PVDF-TiO_2 than PDMS-TiO_2. This result is in great accordance with the photocatalytic efficiency of the above two films under U-L.

3.3 Crystal structure

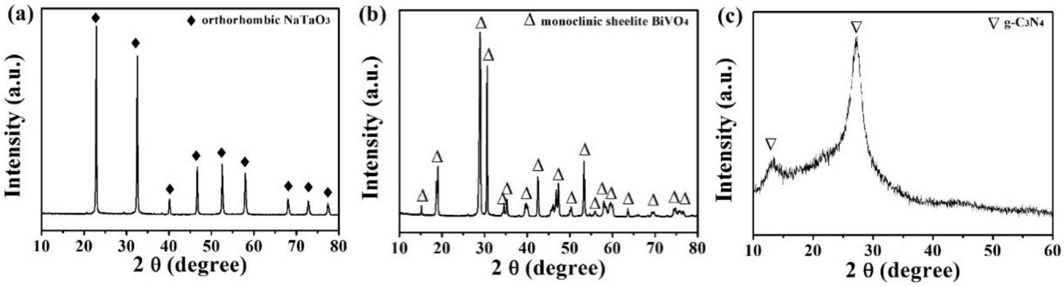

Fig. S3 XRD patterns of the as-synthesized samples: orthorhombic $NaTaO_3$ (a), monoclinic sheelite $BiVO_4$ (b) and g-C_3N_4 (c).

Fig. S3 displays the XRD patterns of the synthesized $NaTaO_3$, $BiVO_4$ and g-C_3N_4 powders. The peaks of $NaTaO_3$ can be well indexed with previously reported cell parameters of orthorhombic $NaTaO_3$,[10, 14] shown in Fig. S3 (a), indicating that the purity $NaTaO_3$ sample is synthesized by hydrothermal method with Ta_2O_5 and NaOH as starting materials. As Fig. S3 (b) depicts, $BiVO_4$ prepared without directing agent is in the form of monoclinic scheelite with the characteristic diffraction peaks at 15.1°, 18.9°, 28.9° and 30.5°.[15] It suggests that the monoclinic sheelite structure of $BiVO_4$ is well preserved in the fabricated sample. Two distinct diffraction peaks of g-C_3N_4 are shown at around 27.4° and 13.1° (Fig. S3 (c)), corresponding to the characterization interplannar staking peak of aromatic systems and the inter-layer structural packing, respectively.[16]

3.4 Morphology characterization

Fig. S4 describes the typical morphologies of the prepared samples $NaTaO_3$, $BiVO_4$ and g-C_3N_4. $NaTaO_3$ is cubic particle with the size less than 200 nm, as Fig. S4 (a) displays. The $BiVO_4$ sample exhibits leaf shape with the thickness of about 300 nm (Fig. S4 (b)). Fig. S4 (c) illustrates the SEM image of the bulk g-C_3N_4, indicating that the obtained g-C_3N_4 sample is solid agglomerate about several micrometers in size.

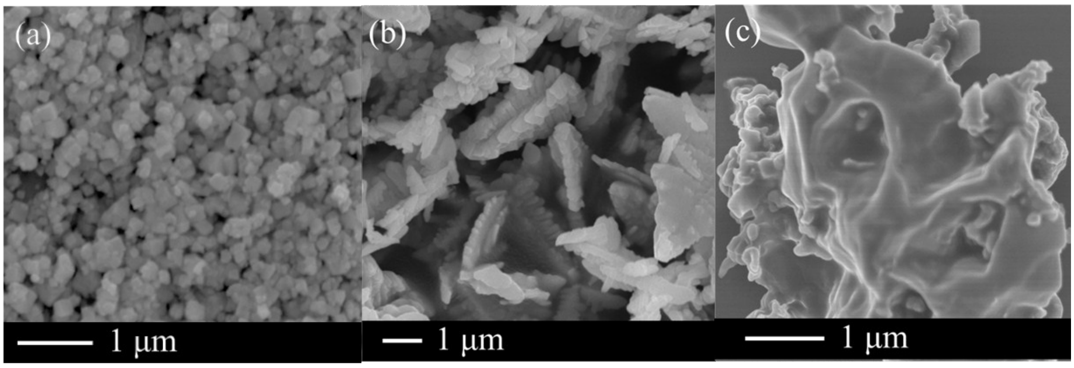

Fig. S4 SEM images of the as-prepared orthorhombic $NaTaO_3$ (a), monoclinic sheelite $BiVO_4$ (b) and g-C_3N_4 (c).

3.5 Optical property

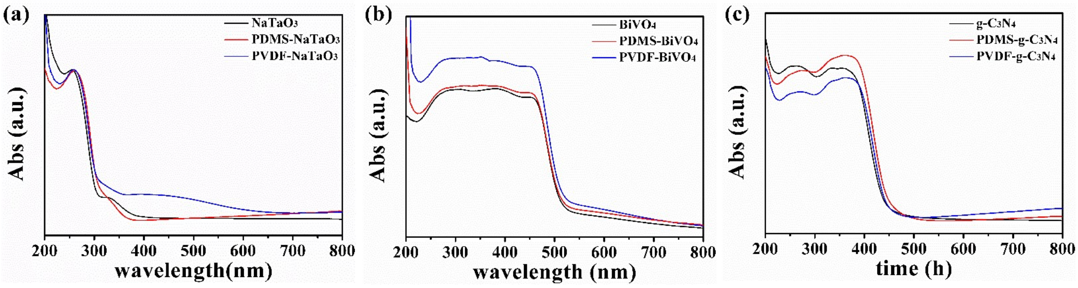

Fig. S5 UV-via absorption spectra of the fabricated powders and films: $NaTaO_3$ powders, PDMS-$NaTaO_3$ and PVDF-$NaTaO_3$ films (a), $BiVO_4$ powders, PDMS-$BiVO_4$ and PVDF-$BiVO_4$ films (b), g-C_3N_4 powders, PDMS-g-C_3N_4 and PVDF-g-C_3N_4 films (c).

As depicted in Fig. S5 (a), (b) and (c), the optical absorptions of $NaTaO_3$, $BiVO_4$ and g-C_3N_4 start at about 320 nm, 530 nm and 450 nm, respectively. The photocatalytic films, PDMS-$NaTaO_3$, PVDF-$NaTaO_3$, PDMS-$BiVO_4$, PVDF-$BiVO_4$, PDMS-g-C_3N_4 and PVDF-g-C_3N_4, possess the same absorption edge as that of the corresponding photocatalyst powders, respectively. Therefore, it allows the prepared photocatalytic films to utilize enough UV light or visible light during the photocatalytic process. The results indicate that the existence of organic substrate PDMS or PVDF does not play a negative role in the light absorption of photocatalyst.

3.6 Generic promotion effect of spatial electric field of PVDF on photocatalysis

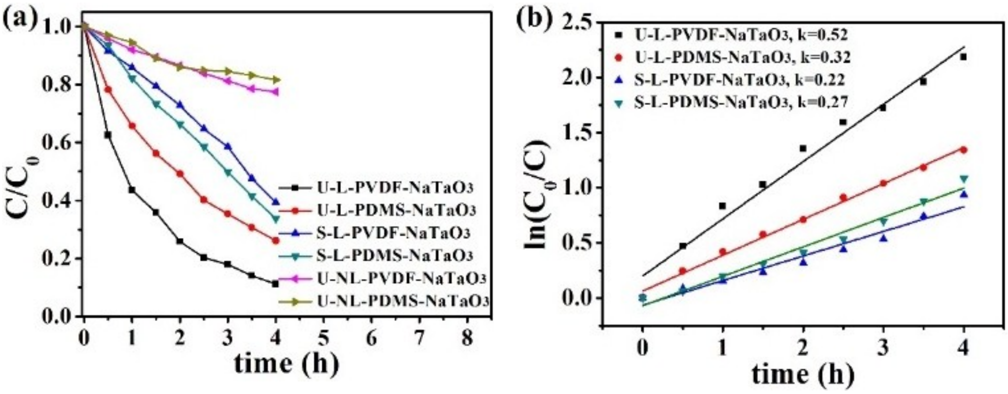

Fig. S6 The photocatalytic degradation curves of RhB (12 mg/L, 100 mL) over PDMS-$NaTaO_3$ film and PVDF-$NaTaO_3$ film under S-L, U-L and U-NL, respectively (a), variations of ln(C_0/C) versus light irradiation time of PDMS-$NaTaO_3$ and PVDF-$NaTaO_3$ films under U-L and S-L, respectively (b).

To investigate whether the spatial electric field of organic PVDF also contributes to improve the photocatalytic activity of other UV-light-responsive photocatalyst or not, the photocatalytic conversions of RhB and K values over the as-prepared PVDF-$NaTaO_3$ and PDMS-$NaTaO_3$ films were studied. Compared with S-L, U-L promotes the photocatalytic activity of PVDF-$NaTaO_3$ by about 30% (from 60% to 90%), and increases its k value by 2.36 times (from 0.22 h^{-1} to 0.52 h^{-1}), presented in Fig. S6. Whereas, without spatial electric field, U-L only improves the photocatalytic activity of PDMS-$NaTaO_3$ by about 10%. There is no great difference in k values of PDMS-$NaTaO_3$ between the condition of U-L (0.32 h^{-1}) and S-L (0.27 h^{-1}). This result implies that spatial electric field of organic PVDF not only accelerates the photocatalysis of TiO_2, but also accelerates the photocatalysis of another UV-light-responsive photocatalyst $NaTaO_3$.

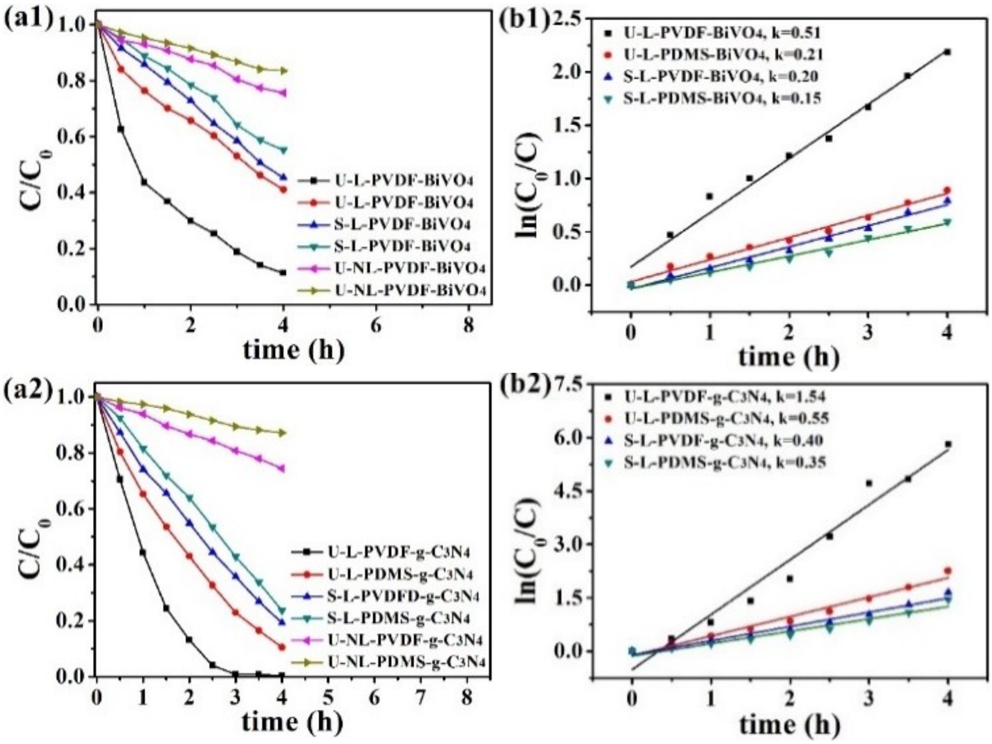

Fig. S7 The photocatalytic degradation curves of RhB (12 mg/L, 100 mL) over PDMS-$BiVO_4$ and PVDF-$BiVO_4$ films (a1), PDMS-g-C_3N_4 and PVDF-g-C_3N_4 films (a2) under S-L, U-L and U-NL, respectively. Variations of $\ln(C_0/C)$ versus light irradiation time of PDMS-$BiVO_4$ and PVDF-$BiVO_4$ films (b1), PDMS-g-C_3N_4 and PVDF-g-C_3N_4 films (b2) under S-L and U-L, respectively.

To further explore the generic enhancement impact of spatial electric field on photocatalysis, two typical visible-light-responsive photocatalysts $BiVO_4$ and g-C_3N_4 were synthesized and combined with PVDF and PDMS substrates, respectively. The catalytic performances of PVDF-$BiVO_4$, PDMS-$BiVO_4$, PVDF-g-C_3N_4 and PDMS-g-C_3N_4 films were studied. As Fig. S7 (a1) and (b1) display, in the presence of U-L, spatial electric field of PVDF improves the photocatalytic efficiency of PVDF-$BiVO_4$ by 35% and increases the corresponding k value by 2.55 times from 0.2 h^{-1} to 0.51 h^{-1}. However, without spatial electric field generated, U-L only boosts the catalytic efficiency of PDMS-$BiVO_4$ by about 15%, which is much lower than 35%. The corresponding k value is also not increased much (0.21 h^{-1} and 0.15 h^{-1} under U-L and S-L, respectively). Moreover, the photocatalytic activities of PVDF-g-C_3N_4 and PDMS-g-C_3N_4 film are accelerated by 35% and 20% in 3 h in the condition of U-L, respectively (Fig. S7 (a2)). The k values of U-L-PVDF-g-C_3N_4 (1.54 h^{-1}) and U-L-PDMS-g-C_3N_4 (0.55 h^{-1}) are 3.85 times and 1.57 times higher than that of S-L-PVDF-g-C_3N_4 (0.40 h^{-1}) and S-L-PDMS-g-C_3N_4 (0.35 h^{-1}), respectively. The increase in k value over PDMS-g-C_3N_4 is not as obvious as that over PVDF-g-C_3N_4, as depicted in Fig. S7 (b2). It indicates that the spatial electric field generated by organic PVDF also plays a promotion role in the photocatalysis of visible-light-responsive photocatalysts, such as $BiVO_4$ and g-C_3N_4. Most significantly, the results provide a strong demonstration that the spatial electric field generated by organic PVDF plays a generic enhancement role in photocatalysis by accelerating charge separation.

References

1 M. Li, P. Li, K. Chang, T. Wang, L. Liu, Q. Kang, S. Ouyang, J. Ye, *Chem. Commun.* 2015, *51*, 7645-7648.

2 D. Xu, W. Shi, C. Song, M. Chen, S. Yang, W. Fan, B. Chen, *Appl. Catal. B: Environ.* 2016, *191*, 228-234.

3 M. Zalfani, B. van der Schueren, Z. Hu, J. C. Rooke, R. Bourguiga, M. Wu, Y. Li, G. Van Tendeloo, B. Su, *J. Mater. Chem. A* 2015, *3*, 21244-21256.

4 B. Yuan, R. Chong, B. Zhang, J. Li, Y. Liu, C. Li, *Chem. Commun.* 2014, *50*, 15593-15596.

5 D. Wang, H. Jiang, X. Zong, Q. Xu, Y. Ma, G. Li, C. Li, *Chem. - A Eur. J.* 2011, *17*, 1275-1282.

6 H. L. Tan, R. Amal, Y. H. Ng, *ACS Appl. Mater. Inter.* 2016, *8*, 28607-28614.

7 S. Cao, J. Low, J. Yu, M. Jaroniec, *Adv. Mater.* 2015, *27*, 2150-2176.

8 P. Niu, L. Zhang, G. Liu, H. Cheng, *Adv. Funct. Mater.* 2012, *22*, 4763-4770.

9 X. Wang, S. Blechert, M. Antonietti, *ACS Catal.* 2012, *2*, 1596-1606.

10 Y. Zhou, Y. Wang, T. Wen, B. Chang, Y. Guo, Z. Lin, B. Yang, *J. Colloid Interf. Sci.* 2016, *461*, 185-194.

11 R. Li, F. Zhang, D. Wang, J. Yang, M. Li, J. Zhu, X. Zhou, H. Han, C. Li, *Nat. Commun.* 2013, *4*, 1432.

12 J. L. G. W. Yuewei Zhang, *Nanoscale* 2012, *4*, 5300–5303.

13 M. Zhang, J. Xu, R. Zong, Y. Zhu, *Appl. Catal. B: Environ.* 2014, *147*, 229-235.

14 X. Li, J. Zang, *J. Phys. Chem. C* 2009, *113*, 19411-19418.

15 D. Wang, R. Li, J. Zhu, J. Shi, J. Han, X. Zong, C. Li, *J. Phys. Chem. C* 2012, *116*, 5082-5089.

16 S. C. Yan, S. B. Lv, Z. S. Li, Z. G. Zou, *Dalton Trans.* 2010, *39*, 1488-1491.